Final Draft
of the original manuscript:

Braune, S.; Basu, S.; Kratz, K.; Johansson, J.B.; Reinthaler, M.; Lendlein, A.;
Jung, F.:

Strategy for the hemocompatibility testing of microparticles

Strategy for the hemocompatibility testing of microparticles

S. Braune[1], S. Basu[1,2], K. Kratz[1], J. Bäckemo Johansson[1], M. Reinthaler[1,3], A. Lendlein[1,2], F. Jung[1]*

1. *Institute of Biomaterial Science and Berlin-Brandenburg Centre for Regenerative Therapies (BCRT), Helmholtz-Zentrum Geesthacht, Teltow, Germany*
2. *Institute of Chemistry, University of Potsdam, Potsdam, Germany*
3. *Department for Cardiology, Charité Universitätsmedizin, Campus Benjamin Franklin, Berlin, Germany*

Corresponding author: F. Jung, friedrich.jung@hzg.de

Abstract

Polymer-based microparticles are applied as non-thrombogenic or thrombogenic materials in a wide variety of intra- or extra-corporeal medical devices. As demanded by the regulatory agencies, the hemocompatibility of these blood contacting biomaterials has to be evaluated *in vitro* to ensure that the particle systems appropriately fulfill the envisioned function without causing undesired events such as thrombosis or inflammation. Currently described *in vitro* assays for hemocompatibility testing of particles comprise tests with different single cell types (e.g. erythrocytes or leukocytes), varying concentrations/dilutions of the used blood cells or whole blood, which are not standardized.

Here, we report about an *in vitro* dynamic test system for studying the hemocompatibility of polymeric microparticles utilizing fresh human whole blood from apparently healthy subjects, collected and processed under standardized conditions. Spherical poly(ether imide) microparticles with an average diameter of 140 ± 30 μm were utilized as model systems. Reported as candidate materials for the removal of uremic toxins, these microparticles are anticipated to facilitate optimal flow conditions in a dialyzer with minimal backflow and blood cell damage. Pristine (PEI) and potassium hydroxide (PEI-KOH) functionalized microparticles exhibited similarly nanoporous surfaces (PEI: $\varnothing_{External\ pore} = 90\pm60$ nm; PEI-KOH $\varnothing_{External\ pore} = 150\pm130$ nm) but varying water wettabilities (PEI: $\theta_{adv} = 112\pm10°$ PEI-KOH $\theta_{adv} = 60\pm2°$). The nanoporosity of the microparticle surfaces allows the exchange of toxic solutes from blood towards the interconnective pores in the particle core, while an immigration of the substantially larger blood cells is inhibited.

Sterilized PEI microparticles were incorporated - air-free - in a syringe-based test system and exposed to whole blood for 60 minutes under gentle agitation. Thereafter, thrombi formation on the particles surfaces were analyzed microscopically. In the collected whole blood the non-adherent/circulating single blood cells were quantified via a differentiated complete blood cell count and the activation of platelets (P-Selectin expression, secretion and release), platelet function (PFA100 closure time) as well as thrombin formation (thrombin-antithrombin-complex) was analyzed. Free hemoglobin (HGB) levels were quantified as a measure of hemolysis.

Microscopic evaluation revealed thrombi formation and particle aggregates for all tested microparticles. Reduction of circulating blood cells differed significantly between the particle types. Particularly, platelet and monocyte counts decreased up to 50% compared to the control (syringe filled with whole blood but without microparticles). In accordance, platelet activation, thrombin levels and degrees of hemolysis were clearly elevated in the particle loaded test systems and allowed a differentiation between the particle types. Increased PFA100 closure times (as activating agent a combination of collagen/ADP was used) indicated a similarly reduced ability of platelets to adhere and form stable aggregates independent from the particle type tested. This observation is most probably a consequence of the strong thrombus formation in the test system, which is associated with a reduction of the circulating blood cells.

The reported *in vitro* dynamic whole blood test system allowed the sensitive analysis of the hemocompatibility of polymer-based microparticles and was successfully validated for porous PEI microparticles with different water wettabilities. Beyond the qualitative and quantitative analysis of cell-material interactions, the test also allowed the functional evaluation of platelets in whole blood.

Introduction

Today, microparticulate biomaterial systems are used for intra- and extracorporeal medical devices [8,16]. Depending on the kind of application, these particles require either thrombogenic or hemocompatible material properties. While thrombogenic particles are applied to induce regeneration in a defined area of the body (e.g. calcium phosphate loaded blood based hydrogels for bone defect filling), hemocompatible microparticles are required for a variety of applications including ultrasound microbubbles, cancer immunotherapy, drug carrier systems and extracorporeal adsorption matrices for the separation or purification of various molecules [1,13,30,35]. To identify and biologically characterize appropriate microparticle systems *in vitro,* hemocompatibility tests have to be performed. Currently described *in vitro* assays for hemocompatibility testing of particles are not standardized and comprise tests with different single cell types (e.g. erythrocytes or leukocytes), varying concentrations/dilutions of the used blood cells or whole blood [20,43]. Such approaches allow studying the interactions between certain cell types and the material properties in a fundamental way and might improve our knowledge about the underlying molecular mechanisms [38]. However, the overall hemocompatibility of the material may only insufficiently be evaluated since the complex interplay and potential signal amplification processes between the different cellular and non-cellular players of the hemostatic and inflammatory system are not considered. Furthermore, the application of varying cell concentrations - e.g. by diluting whole blood differently in the same study - bears the risk of misinterpreting or underestimating dose dependent effects.

Here, we report about an *in vitro* hemocompatibility test, in which fresh human sodium citrated whole blood is utilized for the evaluation of polymer-based microparticles. In order to ensure continuous collisions and interactions between the polymer particles and the different blood cell types, a dynamic test system was chosen based on a gently rotating air-free syringe. The design of the assay allows determining all parameters - such as hemolytic properties of the particles, blood cell retention, soluble signaling proteins and thrombin generation - from the same undiluted fresh human whole blood sample. In a previous study, Tetali et al. confirmed that highly porous poly(ether imide) microparticles are promising absorber materials for the removal of uremic toxins [40]. To evaluate the discriminating power of the introduced whole blood hemocompatibility test, these PEI microparticles as well as modified ones were studied as model systems.

Materials and Methods

Study design

The study protocol was reviewed by the ethics committee of the Charité University Medicine Berlin and in accordance with the ethical guidelines of the journal [9]. The study was designed and performed according to the guidelines of the International Society on Thrombosis and Haemostasis and British committee for standards in haematology [7,18]. According to criteria of the Nordkem-Workshop, blood was taken from apparently healthy subjects, which was free from medication affecting platelet function, for at least 10 days [3]. Donors suffering from lipid metabolism disorder, hypertension or diabetes mellitus were excluded. Blood was withdrawn from the cubital vein following an atraumatic protocol. Blood samples were collected into S-Monovettes® prefilled with sodium citrate ($0.106 \, mol \cdot L^{-1}$, Sarstedt, Germany) or ethylenediaminetetraacetic acid (EDTA, final concentration $1.6 \, mg \cdot mL^{-1}$, Sarstedt, Germany) for blood preanalytics. Immediate homogenization of blood and anticoagulant was ensured by agitation of the collection device during the blood withdrawal. Samples were discarded if clotting was observed. Demographic data of the donors (sex, age, height, weight, body mass index), blood pressure and heart rate were collected. Hemogram data (red- and (differential) white-blood cell count, hemoglobin, hematocrit) were obtained from whole blood (EDTA anticoagulated). Platelet function was tested in the PFA-100® system (Siemens Healthcare Diagnostics, Marburg, Germany) and by flow cytometry (anti human CD42/CD62P antibody positive events) [5,20]. C-reactive protein levels were assessed semi-quantitatively (IMACO, Lüdersdorf, Germany). Subjects were excluded when values were not within the reference ranges for healthy humans, abnormalities in platelet count/function and early inflammatory processes were noticed. Citrated whole blood was allowed to rest for 15 minutes prior any further use.

Poly (ether imide) microparticles

Highly porous poly(ether imide) (PEI) microparticles, exhibiting high surface area, low bulk density and good permeability, were selected as model adsorber particles. Sizes of the spherical shaped particles range between $140 \pm 30 \, \mu m$ and are anticipated to enable optimal flow conditions in the dialyzer with minimal backflow and blood cell damage [42]. Smaller pore sizes at the particle surface ($\varnothing_{External \, pore}$ distribution ~90-200 nm) allow the exchange of toxic solutes from blood towards the larger interconnective pores in the particle core ($\varnothing_{Internal \, pore}$ distribution ~350-500 nm). At the same time, the nanoporosity of the surface prevents the

migration of blood cells into the particle, since the diameter of the external pores deceed the sizes of the smallest cellular blood components at least by the factor 20 (mean diameter of resting platelets: 2-4 µm). PEI particles were functionalized with potassium hydroxide (PEI-KOH) in order to render the porous surface more hydrophilic, which reduces the rapid coating of the particle surfaces with blood plasma proteins as well as the activation of cellular and acellular coagulation pathways, as previously reported [2,29]. Advancing contact angles (θ_{adv}) were found to be substantially reduced from $\theta_{adv} = 112 \pm 10°$ for PEI microparticles to $\theta_{adv} = 60 \pm 2°$ for modified PEI-KOH. High resolution scanning electron microscopy images of the particle surfaces revealed an increase in the mean pore diameter from $\varnothing_{External\ pore} = 90 \pm 60$ nm for PEI microparticles to $\varnothing_{External\ pore} = 150 \pm 130$ nm for PEI-KOH (Figure 1). Internal pore sizes were almost not affected by the functionalization procedure ($\varnothing_{Internal\ pore}$: PEI = 350 ± 90 nm, PEI-KOH = 410 ± 150 nm). This change might be attributed to a pore enlargement/etching at the microparticles surface caused by partial degradation of PEI during the KOH treatment. Cytotoxicity and adsorption capacities of the PEI particles to uremic toxins were tested and reported elsewhere [40]. The results of these studies approved the biocompatibility of the PEI particles. No inflammatory reactions or generation of reactive oxygen species could be determined. Highest absorption affinities were observed for phenylacetic acid and p-cresylsulfate. Indoxyl sulfate and hydroxy hipuric acid showed a partially non-reversible binding.

Hemocompatibility testing of microparticles

Steam-sterilized PEI particles were transferred into sterile syringes (Injekt, B.Braun Melsungen AG, Melsungen, Germany) and equilibrated in sodium chloride (AppliChem, Darmstadt, Germany, room temperature, 24 hours). After withdrawal of the equilibration solution, particles were exposed to whole blood for 60 minutes at room temperature under continuous low agitation (vertical rotation, 5 rpm). Nylon meshes (Falcon Cell strainer, 40 µm, Corning Incorporated, New York, USA) were applied to separate non adherent blood cells from the particles and the surface adherent cells/thrombi. Particles were treated with glutaraldehyde to fix the adherent cells or thrombi [6]. Bright field microscopy (Axio-Imager.Z2m, ZEISS, Zeiss, Jena, Germany) and scanning electron microscopy (Phenom G2 pro, Phenom-World BV, Eindhoven, Netherlands) were carried out to evaluate thrombus formation on the particle surfaces. The complete blood cell count and platelet indices were assessed from EDTA post-anticoagulated whole blood. Measurements were conducted on a SYSMEX 800 (Sysmex XS-800i, SYSMEX Deutschland, Norderstedt, Germany).

Flow cytometry analyses were carried out on a MACSQuant® analyzer (Miltenyi Biotec, Bergisch Gladbach, Germany). Platelets were fixed (Thrombofix platelet stabilizer, Beckman Coulter, Marseille, France) and stained for the GPIb/IX platelet membrane glycoprotein (anti-CD42a-FITC, Becton Dickinson Bioscience, San José CD62P, USA) and the glycoprotein P-Selectin, as marker for the alpha-granules release upon platelet activation (anti-CD62P-PE, Immunotech, Beckman Coulter, Marseille, France) [5].

The PFA-100 (Siemens Healthcare, Erlangen, Germany) was utilized to assess the platelet function in sodium citrated whole blood [11]. Cartridges coated with collagen/ADP were used to measure the closure times after exposition of the particles to the blood.

Platelet Poor Plasma (PPP) was prepared by centrifugation of citrated whole blood (PPP: 1500 g, 20 min). Plasma samples were stored at -80 °C (not longer than 6 months) until the respective ELISA assays were performed. Plasma concentrations of soluble P-Selectin (sP-Selectin) and thrombin–antithrombin III complexes (TAT) were determined with commercially available ELISA assays (sP-Selectin Immunoassay, R&D systems, Wiesbaden-Nordenstadt Germany and Enzygnost® TAT micro, Siemens Healthcare Diagnostics, Marburg, Germany). Free hemoglobin was determined in PPP with a colorimetric method (Diaglobal, Berlin, Germany) [46]. All assays were performed according to the instructions of the manufacturer.

Statistics

For all sampled data, arithmetic mean ± standard deviation are given. For analyzing differences between the PEI particles (including data of the control test system), a one-way ANOVA test was performed with a Tukey adjusted pairwise comparison. P-values less than 0.05 were considered significant. All statistical analyses were carried out in GraphPad Prism version 6.00 for Windows (GraphPad Software, La Jolla, California, USA).

Results and Discussion

In the present study, a dynamic *in vitro* assay was introduced utilizing fresh human whole blood for the hemocompatibility testing of polymer-based microparticles.

Microscopic evaluation of the polymer particles after whole blood exposition and separation of the particles from the non-adherent blood cells revealed a comparable abundance of erythrocyte containing thrombi (red thrombi) on the tested PEI particles (Figure 1). Surface adherent erythrocytes showed normal and intact biconcave discoid morphology and appeared as single cells, small agglutinates or as rouleaux [22].

Aside the reported uremic toxins, further blood plasma proteins might adsorb to the surfaces of the PEI particles inducing adhesion and aggregation of the cells onto the porous surfaces [23,40]. Particularly, the adsorption of fibrinogen was reported for PEI membranes with similar nanoporous surface properties [29] and might enable the interaction of the material surfaces with the erythrocyte membrane via integrin receptors and sialic acids [31].

The quantification of single circulating cells revealed a significant reduction of circulating erythrocytes and platelets and was observed for all polymer particles compared to the control test system (Table 1). Similar results were obtained for the leukocytes, with exception of the basophil counts, which were increased after PEI particle exposure but not significantly different from the values of the control test system. The platelet indices mean platelet volume (MPV) and platelet large cell ratio (P-LCR) differed significantly between the PEI particles and the control test system. No significant differences were observed for the platelet distribution width (PDW). The decrease of the platelet indices after particle exposition to whole blood is presumably associated with higher reactivity of the larger platelets, which are more dense and metabolically more active than smaller platelets [12]. These platelets have a higher thrombotic potential, aggregate preferably and may interact more rapidly with the test materials. This induces the formation of material adherent as well as circulating thrombi and platelet derived microparticles. In a previous study we could show that both processes lead to the decrease of MPV as well as P-LCR values *in vitro,* since the measurement of the platelet volume is limited to single platelets or small platelet aggregates (upper limit for the here applied device: 40 fL) [4].

Pairwise comparisons revealed that differences between PEI particles were significant for the platelet count (PEI versus PEI-KOH; $P<0.05$) but not for the platelet indices. In line with a decreased number of circulating platelets, the percentage of P-Selectin positive platelets and the amount of soluble P-Selectin was lower for PEI-KOH compared to the unmodified PEI (Figure 2). Thrombin generation was significantly increased for PEI-KOH compared to PEI. In concert with the platelet quantification data, this indicates a stronger thrombogenicity of the PEI-KOH particles. Based on these results, we concluded a profound discrimination of the particle thrombogenicity with correlating trends between the above mentioned parameters (Figure 2).

In contrast to the increased level of thrombin generation, PEI-KOH showed the lowest levels of free hemoglobin (0.05 ± 0.02 g·dL^{-1}) while for the unmodified PEI particles the highest degree of hemolysis (0.36 ± 0.07 g·dL^{-1}) was recorded. According to the conventional classification of

hemolyzed specimens, the level of free hemoglobin corresponded to a moderate hemolysis for the PEI particles and a normal or insignificant hemolysis for PEI-KOH and the control test system [26]. Despite differing trends in the particle thrombogenicity and hemolytic properties, determination of hemolysis allowed a sensitive differentiation between the PEI particle types. The percentage of erythrocyte loss was not directly proportional to the percentage of hemolysis. This correlates well with the microscopic data showing intact discoid erythrocytes on the particle surfaces and is in line with previous reports indicating that the hemoglobin release from hemolytic erythrocytes is rather complete (all-or-none leakage) than a partial process (graded leakage) [37].

As reported by Kuroda and others, particularly the hydrophobic nature of a polymer is the dominant factor for its hemolytic activity [24]. Previous reports also indicated that increasing surface hydrophilicity can reduce the polymer-induced hemolysis, most likely by reducing the binding affinity to the erythrocyte membrane [36]. The results of these studies are consistent with our own observations and we concluded that the hydrophobic character of the non-modified PEI surface might be responsible for the elevated hemolytic activity of these particles ($\theta_{adv} = 112\pm10$ °), compared to PEI-KOH particles ($\theta_{adv} = 60\pm 2$ °).

Material surface roughness is considered to predominantly influence blood protein adsorption and adhesion as well as activation of blood cells [27,41]. Previous reports show that a higher surface roughness resulted in an increased available surface area, amplifying adsorption as well as conformational changes of the adsorbed proteins [14,25,33]. Particularly the latter induce platelet adhesion and activation by receptor-mediated recognition of neo or cryptic epitopes, consequently determining the thrombogenicity of a material surface [19]. Based on the higher mean pore diameter at the surface of PEI-KOH particles a higher surface roughness can be anticipated for these particles when compared to the pure PEI microparticles exhibiting a lower mean pore diameter. Besides the change from hydrophobic to hydrophilic wetting behavior after KOH modification, the higher surface roughness of the PEI-KOH particles may be responsible for the higher thrombogenicity of this sample.

Changes in the whole blood closure times after PEI particle exposition displayed significant changes in blood clotting compared to the control test system. This observation was comparable for both tested PEI particles and is very likely associated with the loss of circulating blood cells. Particularly, changes in the hematocrit and plateletcrit, which were observed for both particle types, are reported to induce prolonged clotting times in this device [17,28]. We concluded that this technique is very well suited to indicate global changes, particularly of the platelet function,

but data need to be reconsidered, particularly in view of the complete blood cell count data. The same applies to the microscopic evaluation, which very well allows qualitative judgments of the interaction between blood cells and the materials surface. However, quantification of the surface adherent blood cells might be more appropriately realized by combining the above mentioned indirect measurements of the circulating blood cells with microscopic determination.

In the present study we introduced a dynamic *in vitro* assay utilizing fresh human whole blood for studying the hemocompatibility of blood contacting biomaterials. The test materials are exposed to blood in a closed syringe, which is commercially available, sterile and in medical grade quality. The design of the syringe allows the exclusion of air, which can artificially promote systemic blood activation due to the denaturation of plasma proteins, hemolysis, complement and platelet activation/aggregation during the test procedure [10,32]. In this study, a further modification of the blood-contacting surface - e.g. with heparin - was omitted in order to avoid a potential releasing of the anticoagulant into the tested blood and potential interference with the assay [27,44]. The application of sodium citrate as anticoagulant particularly allowed the assessment of the soluble analytes TAT and sP-Selectin, comparable to the clinical laboratory and at levels, which are reported in clinical studies e.g. for healthy subjects and patients subjected to coronary artery stenting [39,45]. Similarly, complete blood cell count and platelet indices can be linked to the clinical data [15,21]. The good availability and the relatively simple and convenient handling of such test systems may qualify them as good candidates for a more appropriate inter-center and inter-study standardization of hemocompatibility screening assays [34].

Conclusion

The reported *in vitro* whole blood test system allowed the sensitive analysis of the hemocompatibility of polymer-based microparticles and was successfully validated for porous PEI microparticles exhibiting varying water wettabilities. Qualitative and quantitative analysis of cell-material interactions as well as an evaluation of the platelet function in whole blood was demonstrated.

Acknowledgement

References

[1]   T. Balaguer, F. Boukhechba, A. Clavé, S. Bouvet-Gerbettaz, C. Trojani, J.-F. Michiels, J.-P. Laugier, et al., Biphasic calcium phosphate microparticles for bone formation: benefits of combination with blood clot., *Tissue Eng. Part A* **16** (2010), 3495–3505.

[2]   S. Basu, M. Heuchel, T. Weigel, K. Kratz, and A. Lendlein, Integrated process for preparing porous, surface functionalized polyetherimide microparticles, *Polym. Adv. Technol.* **26** (2015), 1447–1455.

[3]   B. Berg, H. Solberg, J. Nilsson, and N. Tryding, Practical experience in the selection and preparation of reference individuals: Empirical testing of the provisional Scandinavian recommendations, in: *Reference values in laboratory medicine*, H. Solberg, R. Grasbeck, T. Alstrom, ed., John Wiley & Sons, Chichester (UK), 1981, 55–64.

[4]   S. Braune, M. Walter, F. Schulze, A. Lendlein, and F. Jung, Changes in platelet morphology and function during 24 hours of storage., *Clin. Hemorheol. Microcirc.* **58** (2014), 159–170.

[5]   S. Braune, M. Von Ruesten-Lange, C. Mrowietz, K. Lützow, T. Roch, A.T. Neffe, A. Lendlein, et al., Dynamic in vitro hemocompatibility testing of poly(ether imide) membranes functionalized with linear, methylated oligoglycerol and oligo(ethylene glycol), *Clin. Hemorheol. Microcirc.* **54** (2013), 235–248.

[6]   S. Braune, M. Groß, M. Walter, S. Zhou, S. Dietze, S. Rutschow, A. Lendlein, et al., Adhesion and activation of platelets from subjects with coronary artery disease and apparently healthy individuals on biomaterials, *J. Biomed. Mater. Res. B. Appl. Biomater.* **104** (2016), 210–217.

[7]   M. Cattaneo, C. Cerletti, P. Harrison, C.P.M. Hayward, D. Kenny, D. Nugent, P. Nurden, et al., Recommendations for the Standardization of Light Transmission Aggregometry: A Consensus of the Working Party from the Platelet Physiology Subcommittee of SSC/ISTH., *J. Thromb. Haemost.* **11** (2013), 1183–1189.

[8]   W.-K. Cheah, K. Ishikawa, R. Othman, and F.-Y. Yeoh, Nanoporous biomaterials for uremic toxin adsorption in artificial kidney systems: A review, *J. Biomed. Mater. Res. B. Appl. Biomater.* (2016), Epub ahead of print.

[9]   Editorial board of the journal Clinical Hemorheology and Microcirculation, Ethical guidelines for publication in Clinical Hemorheology and Microcirculation: Update 2016, *Clin. Hemorheol. Microcirc.* **63** (2016), 1–2.

[10]   A.M. El-Sabbagh, C.J. Toomasian, J.M. Toomasian, G. Ulysse, T. Major, and R.H. Bartlett, Effect of air exposure and suction on blood cell activation and hemolysis in an in vitro cardiotomy suction model., *ASAIO J.* **59** (2013), 474–479.

[11]   E.J. Favaloro, Clinical utility of the PFA-100., *Semin. Thromb. Hemost.* **34** (2008), 709–733.

[12] M.K. Freynhofer, S.C. Gruber, E.L. Grove, T.W. Weiss, J. Wojta, and K. Huber, Antiplatelet drugs in patients with enhanced platelet turnover: biomarkers versus platelet function testing, *Thromb. Haemost.* **114** (2015), 459–468.

[13] S. Geis, L. Prantl, M. Schoeneich, P. Lamby, S. Klein, J. Dolderer, S. Mueller, et al., Contrast enhanced ultrasound (CEUS) – an unique monitoring technique to assess microvascularization after buried flap transplantation, *Clin. Hemorheol. Microcirc.* **62** (2016), 205–214.

[14] K. Gester, S. Birtel, J. Clauser, U. Steinseifer, and S.J. Sonntag, Real-Time Visualization of Platelet Interaction With Micro Structured Surfaces, *Artif. Organs* **40** (2016), 201–207.

[15] T.V. Giovanetti, A.J. Do Nascimento, and J.P. De Paula, Platelet indices, *Rev. Bras. Hematol. Hemoter.* **33** (2011), 164–165.

[16] L. Gu and D.J. Mooney, Biomaterials and emerging anticancer therapeutics: engineering the microenvironment., *Nat. Rev. Cancer* **16** (2015), 56–66.

[17] P.A. Gurbel, R.C. Becker, K.G. Mann, S.R. Steinhubl, and A.D. Michelson, Platelet function monitoring in patients with coronary artery disease., *J. Am. Coll. Cardiol.* **50** (2007), 1822–1834.

[18] P. Harrison, I. Mackie, A. Mumford, C. Briggs, R. Liesner, M. Winter, and S. Machin, Guidelines for the laboratory investigation of heritable disorders of platelet function., *Br. J. Haematol.* **155** (2011), 30–44.

[19] D.M. Hylton, S.W. Shalaby, and R.A. Latour, Direct correlation between adsorption-induced changes in protein structure and platelet adhesion, *J. Biomed. Mater. Res. A* **73** (2005), 349–358.

[20] F. Jung and S. Braune, Thrombogenicity and hemocompatibility of biomaterials, *Biointerphases* **11** (2016), 29601.

[21] K. Kaito, H. Otsubo, N. Usui, M. Yoshida, J. Tanno, E. Kurihara, K. Matsumoto, et al., Platelet size deviation width, platelet large cell ratio, and mean platelet volume have sufficient sensitivity and specificity in the diagnosis of immune thrombocytopenia, *Br. J. Haematol.* **128** (2005), 698–702.

[22] E. Kaliviotis, J. Dusting, J.M. Sherwood, and S. Balabani, Quantifying local characteristics of velocity, aggregation and hematocrit of human erythrocytes in a microchannel flow, *Clin. Hemorheol. Microcirc.* **63** (2015), 123–148.

[23] R.K. Kumar, S. Basu, H.D. Lemke, J. Jankowski, K. Kratz, A. Lendlein, and S.D. Tetali, Effect of extracts of poly(ether imide) microparticles on cytotoxicity, ROS generation and proinflammatory effects on human monocytic (THP-1) cells, *Clin. Hemorheol. Microcirc.* **61** (2016), 667–680.

[24] K. Kuroda, G.A. Caputo, and W.F. DeGrado, The role of hydrophobicity in the antimicrobial and hemolytic activities of polymethacrylate derivatives, *Chem. - A Eur. J.* **15** (2009), 1123–1133.

[25] J. Linneweber, P.M. Dohmen, U. Kertzscher, U. Kerzscher, K. Affeld, Y. Nosé, and W. Konertz, The effect of surface roughness on activation of the coagulation system and platelet adhesion in rotary blood pumps, *Artif. Organs* **31** (2007), 345–351.

[26]   G. Lippi, Systematic Assessment of the Hemolysis Index, in: 2015, 157–170.

[27]   X. Liu, L. Yuan, D. Li, Z. Tang, Y. Wang, G. Chen, H. Chen, et al., Blood compatible materials: state of the art, *J. Mater. Chem. B* **2** (2014), 5718.

[28]   M. Lordkipanidzé, Platelet Function Tests., *Semin. Thromb. Hemost.* **42** (2016), 258–267.

[29]   A.T. Neffe, M. von Ruesten-Lange, S. Braune, K. Lützow, T. Roch, K. Richau, A. Krüger, et al., Multivalent grafting of hyperbranched oligo- and polyglycerols shielding rough membranes to mediate hemocompatibility, *J. Mater. Chem. B* **2** (2014), 3626–3635.

[30]   A.T. Neffe, C. Wischke, M. Racheva, and A. Lendlein, Progress in biopolymer-based biomaterials and their application in controlled drug delivery, *Expert Rev. Med. Devices* **10** (2013), 813–833.

[31]   S. De Oliveira, V.V. De Almeida, A. Calado, H.S. Rosário, and C. Saldanha, Integrin-associated protein (CD47) is a putative mediator for soluble fibrinogen interaction with human red blood cells membrane, *Biochim. Biophys. Acta - Biomembr.* **1818** (2012), 481–490.

[32]   J.R. Pohlmann, J.M. Toomasian, C.E. Hampton, K.E. Cook, G.M. Annich, and R.H. Bartlett, The relationships between air exposure, negative pressure, and hemolysis., *ASAIO J.* **55** (2009), 469–473.

[33]   K. Rechendorff, M.B. Hovgaard, M. Foss, V.P. Zhdanov, and F. Besenbacher, Enhancement of protein adsorption induced by surface roughness., *Langmuir* **22** (2006), 10885–10888.

[34]   I. Reviakine, F. Jung, S. Braune, J.L. Brash, R. Latour, M. Gorbet, and W. van Oeveren, Stirred, shaken, or stagnant: What goes on at the blood–biomaterial interface, *Blood Rev.* (2016), doi: 10.1016/j.blre.2016.07.003.

[35]   R.E. Serda, Particle platforms for cancer immunotherapy, *Int. J. Nanomedicine* **8** (2013), 1683–1696.

[36]   J. Shi, Y. Hedberg, M. Lundin, I. Odnevall Wallinder, H.L. Karlsson, and L. Möller, Hemolytic properties of synthetic nano- and porous silica particles: The effect of surface properties and the protection by the plasma corona, *Acta Biomater.* **8** (2012), 3478–3490.

[37]   I. Sovadinova, E.F. Palermo, R. Huang, L.M. Thoma, and K. Kuroda, Mechanism of polymer-induced hemolysis: Nanosized pore formation and osmotic lysis, *Biomacromolecules* **12** (2011), 260–268.

[38]   C. Sperling, R.B. Schweiss, U. Streller, and C. Werner, In vitro hemocompatibility of self-assembled monolayers displaying various functional groups, *Biomaterials* **26** (2005), 6547–6557.

[39]   K. Takada, S. Ishikawa, N. Yokoyama, N. Hosogoe, and T. Isshiki, Effects of eicosapentaenoic acid on platelet function in patients taking long-term aspirin following coronary stent implantation., *Int. Heart J.* **55** (2014), 228–233.

[40]   S.D. Tetali, V. Jankowski, K. Luetzow, K. Kratz, A. Lendlein, and J. Jankowski, Adsorption capacity of poly(ether imide) microparticles to uremic toxins, *Clin.*

Hemorheol. Microcirc. **61** (2016), 657–665.

[41]   A.A. Thyparambil, Y. Wei, and R.A. Latour, Experimental characterization of adsorbed protein orientation, conformation, and bioactivity, *Biointerphases* **10** (2015), 19002.

[42]   U. Tschulena, G. Reinhold, J. Passlick-Deetjen, H. P. Leinenbach, A. Hörberg, and K. Oleschko, "Adsorber granules for removing uraemic toxins." 2015

[43]   J. Vienken, Biomaterials for medical devices: Are current hemo- or biocompatibility tests adequate?. Biomaterialien für Medizinprodukte: Testen wir richtig?, *Materwiss. Werksttech.* **41** (2010), 1081–1085.

[44]   H. Wendel, N. Weber, and G. Ziemer, Adsorption of Plasma Proteins at Heparin-Coated Surfaces - Comparative Investigations, *Biomed. Tech.* **45** (2000), 282–287.

[45]   J.J. Wykrzykowska, A. Warnholtz, P. de Jaeger, N. Curzen, K.G. Oldroyd, J.P. Collet, J.M. Ten Berg, et al., Effect of clopidogrel discontinuation at 1 year after drug eluting stent placement on soluble CD40L, P-selectin and C-reactive protein levels: DECADES (Discontinuation Effect of Clopidogrel After Drug Eluting Stent): A multicenter, open-label study, *J. Thromb. Thrombolysis* **28** (2009), 410–417.

[46]   A. Zwart, O.W. van Assendelft, B.S. Bull, J.M. England, S.M. Lewis, and W.G. Zijlstra, Recommendations for reference method for haemoglobinometry in human blood (ICSH standard 1995) and specifications for international haemiglobinocyanide standard (4th edition)., *J. Clin. Pathol.* **49** (1996), 271–274.
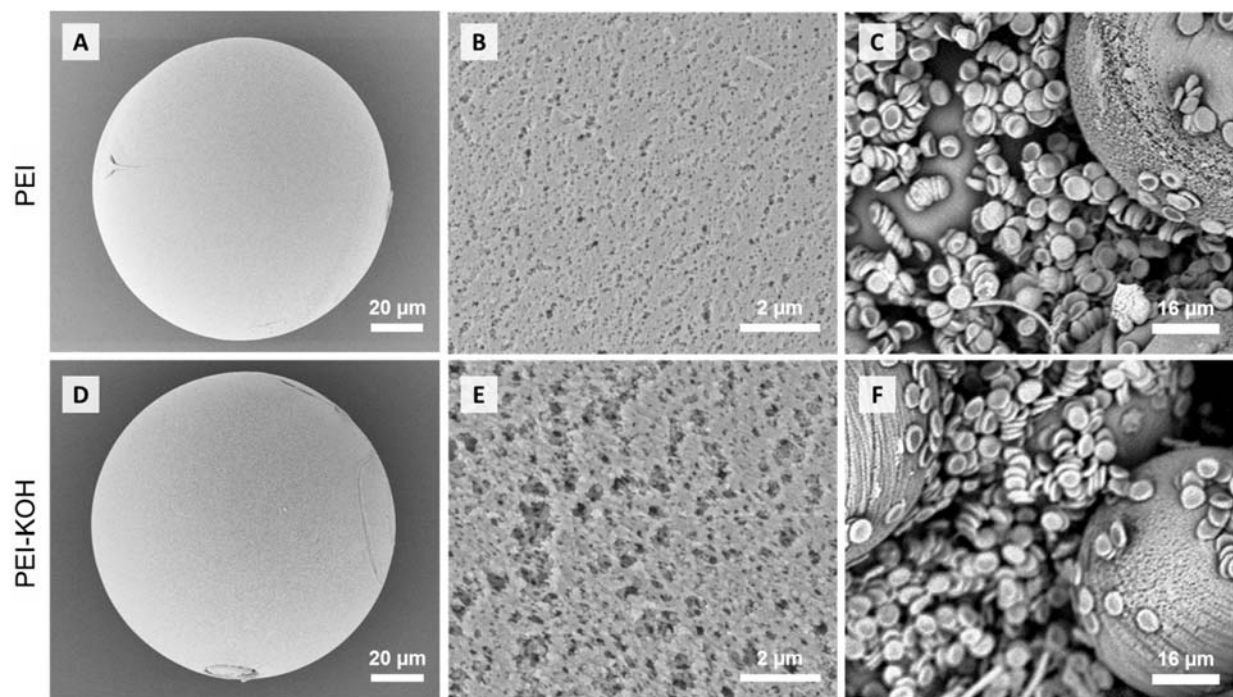
Figures and tables

Figure 1. Representative microscopic images of PEI microparticles A and D: Topview on single particles; B and E: Detail image of particle surfaces; C and F: PEI particles after whole-blood exposition (scanning electron microscopy).

Table 1. Complete blood cell count and platelet indices (Data are given as arithmetic mean ± standard deviation, P values are results of a one way ANOVA test including all particle types and the control test system).

| Parameter	Unit	Control	PEI	PEI-KOH	P value
Erythrocytes	$10^4 \cdot \mu L^{-1}$	491.2 ± 62.1	416,8 ± 53,4	438,8 ± 83,5	0.04
Total Leukocytes	$10^1 \cdot \mu L^{-1}$	513.3 ± 140.3	382,2 ± 122,2	363,5 ± 127,5	<0.01
Neutrophils	$10^1 \cdot \mu L^{-1}$	329.0 ± 132.3	243,2 ± 112,5	226,0 ± 109,1	<0.01
Lymphocytes	$10^1 \cdot \mu L^{-1}$	127.3 ± 23.3	107,7 ± 21,3	110,3 ± 24,7	<0.01
Monocytes	$10^1 \cdot \mu L^{-1}$	39,8 ± 8,4	16,2 ± 5,3	13,8 ± 5,8	<0.01
Eosinophils	$10^1 \cdot \mu L^{-1}$	16,3 ± 11,9	12,5 ± 8,6	11,3 ± 9,5	0.02
Basophils	$10^1 \cdot \mu L^{-1}$	0,8 ± 0,4	2,7 ± 1,4	2,0 ± 1,4	0.08
Platelets	$10^3 \cdot \mu L^{-1}$	175,0 ± 41,7	103,0 ± 12,1	63,0 ± 28,9	<0.01
Mean platelet volume	fL	10,6 ± 0,6	10,1 ± 0,8	9,9 ± 0,5	<0.01
Platelet large cell ratio	%	30,8 ± 4,7	27,3 ± 5,6	26,6 ± 4,2	<0.01
Platelet distribution width	fL	13,1 ± 1,2	12,8 ± 1,7	12,5 ± 1,2	0.41
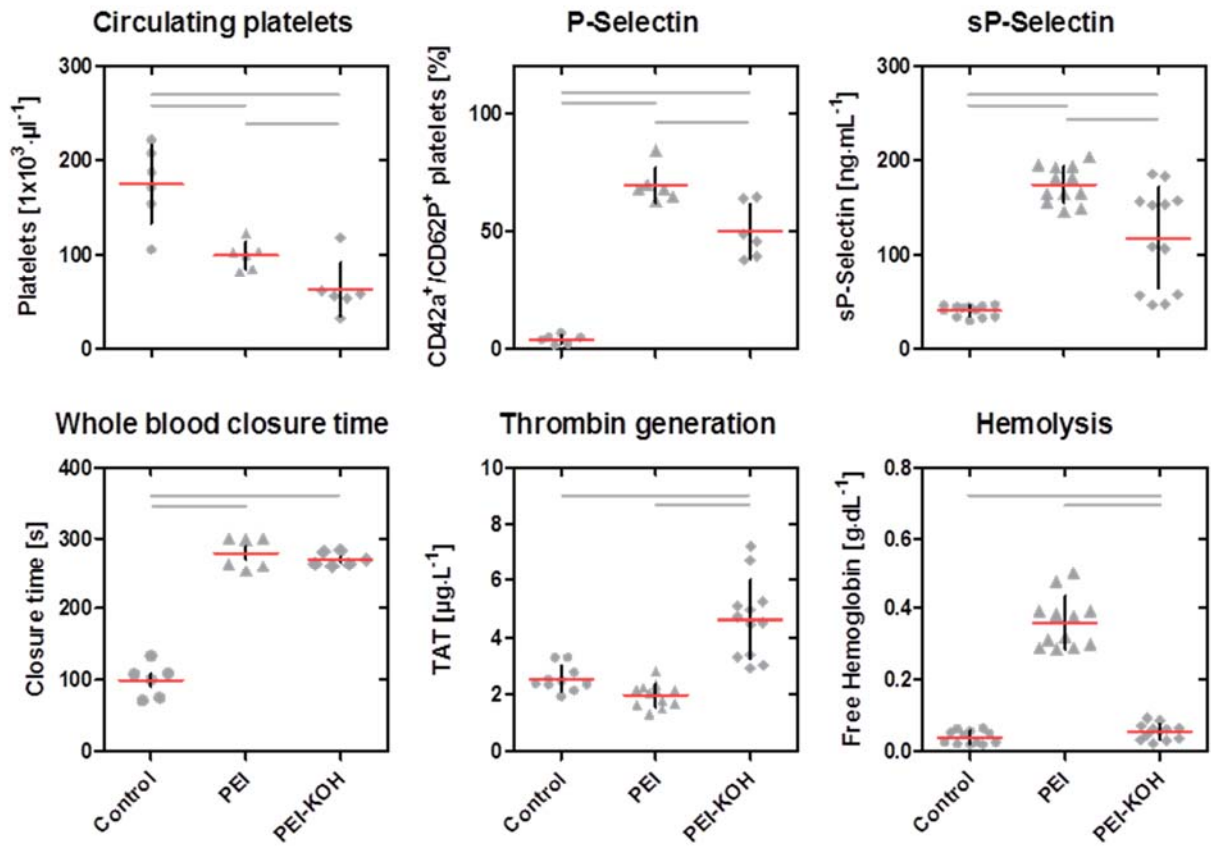
Figure 2. Platelet function, thrombi generation and hemolysis analyses (Control = empty test system, arithmetic mean = horizontal red bar, standard deviation = vertical black bar, grey bars = p<0.05 ANOVA).